Carbohydrate Polymers 108 (2014) 83–90

Contents lists available at ScienceDirect

Carbohydrate Polymers

journal homepage: www.elsevier.com/locate/carbpol

Preparation and properties of carboxymethyl cellulose/layered double hydroxide bionanocomposite films

Mehdi Yadollahi [a], Hassan Namazi [a,b,*], Soroush Barkhordari [a]

[a] Research Laboratory of Dendrimers and Nanopolymers, Faculty of Chemistry, University of Tabriz, P.O. Box 51666, Tabriz, Iran
[b] Research Center for Pharmaceutical Nanonotechnology, Tabriz University of Medical Science, Tabriz, Iran

ARTICLE INFO

Article history:
Received 31 October 2013
Received in revised form 3 March 2014
Accepted 11 March 2014
Available online 22 March 2014

Keywords:
Bionanocomposite
Carboxymethyl cellulose
Layered double hydroxide
Anionic clays

ABSTRACT

Solution casting method was employed for preparing of carboxymethyl cellulose/layered double hydroxide (CMC–LDH) bionanocomposite films with LDH content ranged from 0 to 8 wt%. The synthesized nanocomposite films were characterized using FTIR, XRD, TEM and SEM analytical methods. XRD and TEM analysis revealed a partially exfoliated structure for nanocomposites with LDH content up to 3 wt%. However, for LDH contents higher than 3 wt%, nanocomposites formed an intercalated structure. Incorporation of LDH significantly decreased water vapor permeability (WVP) of the bionanocomposite films up to 37%. Addition of the LDHs into the CMC matrix is accompanied by a decrease in the film transparency. Mechanical properties of CMC-based films were improved significantly by addition of LDH particles. CMC–LDH nanocomposite film with 3 wt% LDH showed a 148 and 143% increase in the tensile strength and tensile modulus, as well as a 62% decrease in elongation in comparison with the pure CMC film.

1. Introduction

Polymer nanocomposites are a new generation of materials that contain a polymeric matrix and less than 10% by weight of a nanoscale reinforcing particle. The polymer nanocomposites have better interaction with filler compared with the conventional composites. Uniform distribution of nanoparticles in the polymer matrix causes an improvement of the mechanical, thermal, and gas barrier properties of composites (Pavlidou & Papaspyrides, 2008). Bio-nanocomposites are an emerging class of composites that formed by the combination of a natural polymer and an inorganic or organic nanoparticle. These nanocomposites have attracted much attention in medicine and environmentally friendly materials because of their desirable properties such as biocompatibility and biodegradability (Zhao, Torley, & Halley, 2008).

Among various nanofillers, nanoparticles with a large aspect ratio have proven to be more impressive in polymer matrix reinforcement, such as layered silicates (Namazi, Dadkhah, & Mosadegh, 2012; Namazi, Mosadegh, & Dadkhah, 2009), carbon nanotubes (Chen, Goren, Ozisik, & Schadler, 2012; Shawky, Chae, Lin, & Wiesner, 2011), cellulose nanocrystals (Bitinis et al., 2013; Eichhorn, 2011) and graphite nanoplatelets (El Achaby et al., 2012; Galpaya et al., 2012). Recently, another type of inorganic nanoparticle, layered double hydroxides (LDHs), otherwise called anionic clays, and their intercalation compounds has aroused much attention. LDHs have been used as catalysts, ion exchangers, optical hosts, ceramic precursors and in the preparation of polymer nanocomposites (Kuang et al., 2010; Zümreoglu-Karan & Ay, 2012). In comparison to layered silicates, the LDH structure consists of positively charged brucite-like $[M(OH)_2]$ sheets containing both bivalent and trivalent cations and anions within interlayer galleries. LDHs are represented by the general formula $[M^{2+}{}_{1-x}M^{3+}{}_x(OH)_2]^{x+}\cdot[(An^{m-})_{x/m}\cdot yH_2O]$ with representative examples M^{2+} = Mg, Zn or Ca; M^{3+} = Al, Cr or Fe; An^{m-} = $CO_3{}^{2-}$, $C1^-$, OH^-, $NO_3{}^-$ or $SO_4{}^{2-}$, and x taking values between 0.2 and 0.4 (Wang & O'Hare, 2012).

The facile synthesis, versatility and flexibility in composition, biodegradability and biocompatibility of LDHs, makes them, especially attractive in the preparation of bio-nanocomposites and other types of biohybrid materials (Hitzky, Darder, Aranda, & Ariga, 2010; Zhao et al., 2008). Recently, several biopolymers such as casein (Yu, Bian, & Plank, 2010), deoxyribonucleic acid (DNA) (Choy, Kwak, Park, Jeong, & Portier, 1999; Desigaux et al., 2006; Oh, Kwak, & Choy, 2006) and polysaccharides like starch (Chung & Lai, 2010; Wu, Chang, & Ma, 2011), alginate (Alcantara, Aranda, Darder, & Ruiz-Hitzky, 2010; Darder, López-Blanco, Aranda, Leroux, & Ruiz-Hitzky, 2005; Leroux, Gachon, & Besse, 2004; Mandal, Patil, & Mayadevi, 2012), pectin (Darder et al., 2005; Gorrasi, Bugatti, & Vittoria, 2012)

* Corresponding author at: Research Laboratory of Dendrimers and Nanopolymers, Faculty of Chemistry, University of Tabriz, P.O. Box 51666, Tabriz, Iran. Tel.: +98 4113393121.
E-mail address: namazi@tabrizu.ac.ir (H. Namazi).

http://dx.doi.org/10.1016/j.carbpol.2014.03.024
0144-8617/

and i-carrageenan (Darder et al., 2005) have also been successfully intercalated into LDH phases using ion exchange, co-precipitation, delamination-restacking and reconstruction methods.

Carboxymethyl cellulose (CMC) is an anionic, water-soluble cellulose derivative obtained by introducing $-CH_2COOH$ groups into cellulose molecular chain. It has received much interest due to its unique properties such as high viscosity, transparency, hydrophilicity, non-toxic, biocompatibility, biodegradability and good film forming ability. It has been employed for several applications such as drug delivery, textile printing, paper industry, detergents, food, and oil well drilling operations among others (Heinze, Liebert, Klüfers, & Meister, 1999; Stigsson, Kloow, & Germgård, 2006; Wang & Somasundaran, 2005; Yang & Zhu, 2007). To improve its properties, different nano-particles such as copper complexes (Basta & El-Saied, 2008), silver nanoparticles (Singh & Ahmad, 2012; Song, Birbach, & Hinestroza, 2012), Cellulose nanocrystal (Choi & Simonsen, 2006), hydroxyapatite (Zakharov, Ezhova, Kalinnikov, & Chalykh, 2005), calcium carbonate (Shen, Song, Qian, & Yang, 2010), Fe_3O_4 (Chang, Yu, Ma, & Anderson, 2011) and ZnS (Luna-Martinez et al., 2011) and graphene oxide (Yadav, Rhee, Jung, & Park, 2013) have been incorporated into CMC matrix. According to the best of our knowledge, a few reports have been published on using LDHs for preparation CMC–LDH nanocomposites (Kang et al., 2009; Yadollahi & Namazi, 2013). For instance, Kang et al., have prepared CMC–LDH intercalated nanocomposites through coassembly of layered double hydroxide (LDH) nanosheets with carboxymethyl cellulose. They reported a significant enhancement in the thermal stability of CMC after preparation of CMC–LDH nanocomposite (Kang et al., 2009). Additionally, in our previous work (Yadollahi & Namazi, 2013); we reported preparation of CMC–LDH intercalated nanocomposites through co-precipitation method. The obtained nanocomposites revealed a better thermal stability and a pH dependent swelling behavior.

In this study, we describe the synthesis and characterization of carboxymethyl cellulose/LDH exfoliated nanocomposite films by casting CMC and LDH aqueous solution. The microstructures, mechanical and thermal, optical and barrier properties of CMC/LDH nanocomposites films were examined a function of LDH concentration by X-ray diffraction (XRD), TEM, SEM analysis, UV–vis, water vapor permeability and mechanical tests. The LDH concentration of the nanocomposite films ranged from 0 to 8 wt%.

2. Experimental

2.1. Materials

Sodium carboxymethyl cellulose (CMC), degree of substitution (DS) 0.55–1.0 and viscosity 15,000 mPas/s (1% in H2O, 25 °C) was obtained from Nippon Paper Chemicals Co., Ltd., Japan. $Mg(NO_3)_2{\cdot}6H_2O$, $Al(NO_3)_3{\cdot}9H_2O$ and NaOH and glycerol were purchased from Merck. All the chemicals were used as received without further purification. Bi-distilled water was used throughout this work.

2.2. Preparation of LDH

Mg–Al-LDH was prepared by co-precipitation method. First, an aqueous solution (50 ml) of $Mg(NO_3)_2{\cdot}6H_2O$ (33.5 mmol) and $Al(NO_3)_3{\cdot}9H_2O$ (16.5 mmol) was prepared, followed by drop-wise addition of NaOH solution (50 ml, 2 M) with constant stirring under N_2 atmosphere. Afterwards, the slurry was aged for 24 h at 95 °C, keeping the pH at 9–10 by adjusting with NaOH (2.0 M) solution. After washing, the wet sample was divided into two portions. One portion was dried at 50 °C under vacuum for 24 h. Another portion was dispersed in water and subjected to ultrasonic irradiation for 10 min at full power to disperse the LDH particles. The LDH content in the colloidal dispersion was measured by air drying (3%, w/w). The suspension was used directly in our experiments.

2.3. Preparation of CMC–LDH nanocomposite films

CMC–LDH bionanocomposite films with 1, 3, 5 and 8 wt% were prepared by a casting/evaporation method as follows: typically, 2 g CMC and desired amount of LDH suspension contains 0.02–0.16 g LDH and 1 g of glycerol were added into 100 ml bi-distilled water. A homogeneous solution was obtained by constant stirring of the mixture at 90 °C for 24 h. The solution was then subjected to ultrasonic irradiation for 10 min at full power to disperse the LDH particles and reduce aggregation. Then, the obtained homogenous solution was poured into a Teflon mold (18 cm × 18 cm) and heated to 50 °C for approximately 24 h to evaporate water. After drying, the films were removed from the mold and different of analytical tests were carried on them.

2.4. Film characterization

Infrared spectra were obtained on an FTIR spectrometer (Bruker Instruments, model Aquinox 55, Germany) in the 4000–400 cm^{-1} range at a resolution of 0.5 cm^{-1} as KBr pellets. UV–vis spectroscopy was carried out on a Perkin-Elmer Lambda 35 UV–vis absorption spectrometer at room temperature. The X-ray diffraction patterns of the samples were obtained by Siemens diffractometer with Cu-Kα radiation at 35 kV in the scan range of 2θ from 2 to 70°. All of analyzed samples were in powdery form. The d-spacing was calculated by Bragg's equation where λ was 0.154 nm. Transmission electron micrograph (TEM) was conducted by LEO 906E transmission electron microscope operating at 80 kV. Scanning electron micrographs (SEM) were obtained with LEO 1430VP scanning electron microscope operating at 15 kV. Tensile properties of free films were investigated by a universal test machine (MTS, model 10/M, USA) according to ISO 527 at room temperature. Five films were cut into 2 cm × 15 cm strips. Films were held parallel with an initial grip separation of 10 cm and pulled apart at a head speed of 25 mm/min.

Water vapor permeability of films (g m^{-1} h^{-1} Pa^{-1}) was gravimetrically determined at 20 °C using a method described by Tunc et al. (2007). Prepared nanocomposite films were hermetically sealed with silicone grease in glass cups (4.8 cm × 3.8 cm × 4.0 cm) containing 15 ml distilled water. The cups were placed at 20 °C in desiccators containing silicagel, thus obtaining an RH gradient equal to 100%. The water vapor transfer through the exposed film area (18.24 cm^2) was measured from the cup weight loss as a function of time. The cups were weighed using a four-digit balance every 24 h over a 5-day period, after steady-state vapor flow had been reached. At least three samples of each type of film were tested, and water vapor permeability (WVP) was calculated from the following equation:

$$\mathrm{WVP} = \frac{S \times d}{A \times \Delta P}$$

where S is the slope of the weight loss versus time (g h^{-1}), d is the film thickness (m), A is the area of exposed film (m^2) and ΔP is the differential of water vapor pressure across the film (at 20 °C, $\Delta P = 2.33 \times 103$ Pa, assuming that the RH on the silicagel is negligible).

3. Results and discussions

3.1. FTIR analysis

Fig. 1 illustrates the corresponding FTIR spectra for CMC film, the pristine Mg–Al-LDH and CMC–LDH nanocomposite film with

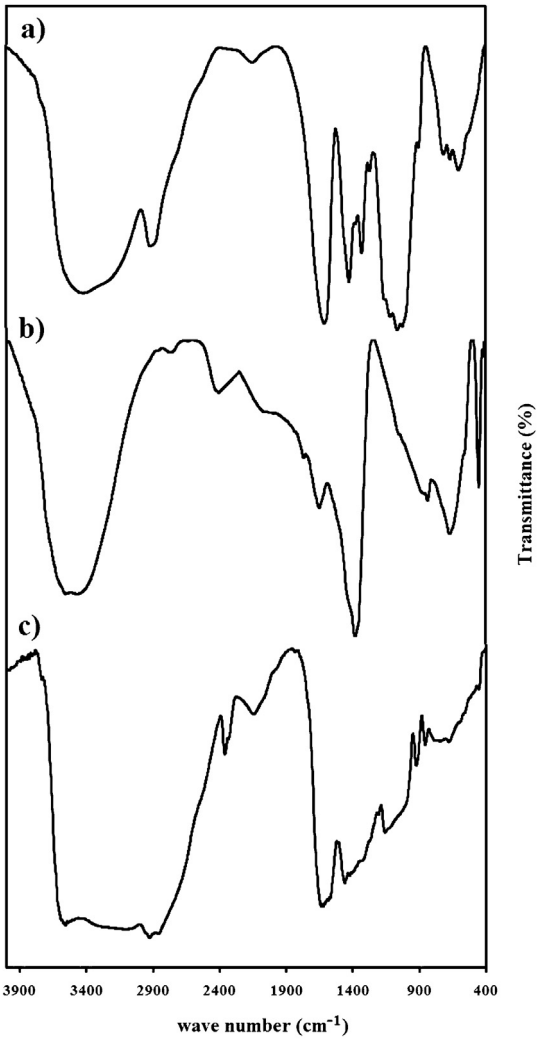

Fig. 1. FTIR spectra of (a) CMC film (b) Mg–Al-LDH (c) CMC–LDH nanocomposite film.

8 wt% LDH content in the 4000–400 cm^{-1} wave number range. The FTIR spectra of CMC film exhibited the broad band centered at 3420 cm^{-1}, attributed to the stretching of–OH groups and intermolecular and intramolecular hydrogen bonds. And the peak about C—H stretching associated with the methane hydrogen atoms appeared at 2913 cm^{-1}. The peaks at 1422 and 1607 cm^{-1} were related to the symmetrical and asymmetrical stretching vibrations of the carboxylate groups. The absorption bands between 1000 and 1200 cm^{-1} were ascribed to the —C—O— stretching on the polysaccharide skeleton (Luna-Martinez et al., 2011; Wu et al., 2011).

The FTIR spectra for Mg–Al-LDH can be seen in Fig. 2b. In the spectrum of Mg–Al-LDH), it was observed an absorption band at around 3500 cm^{-1} due to the OH stretching of hydroxyl group and water molecules present in the interlayer space of LDH. The corresponding bending vibration mode of water molecules appears around 1623 cm^{-1}. A strong peak at 1380 cm^{-1} appeared in the spectra of Mg–Al-LDH is associated with the characteristic peak of NO_3 interlayer anions. The peaks and bonds in the 400–800 cm^{-1} region are associated with M—O and O—M—O (M=Mg and Al) stretching modes in the LDHs sheets (Olanrewaju, Newalkar, Mancino, & Komarneni, 2000).

The FTIR spectra of the CMC–LDH nanocomposite film represents two types of bands: one corresponding to the CMC matrix and the other related to the LDH sheets. Compared with the FTIR spectra of CMC film, CMC–LDH film indicates the new peaks in the 400–800 cm^{-1} regions. These peaks were attributed to the vibration bands of LDH sheets arising from M—O and O—M—O bonds (Yadollahi & Namazi, 2013).

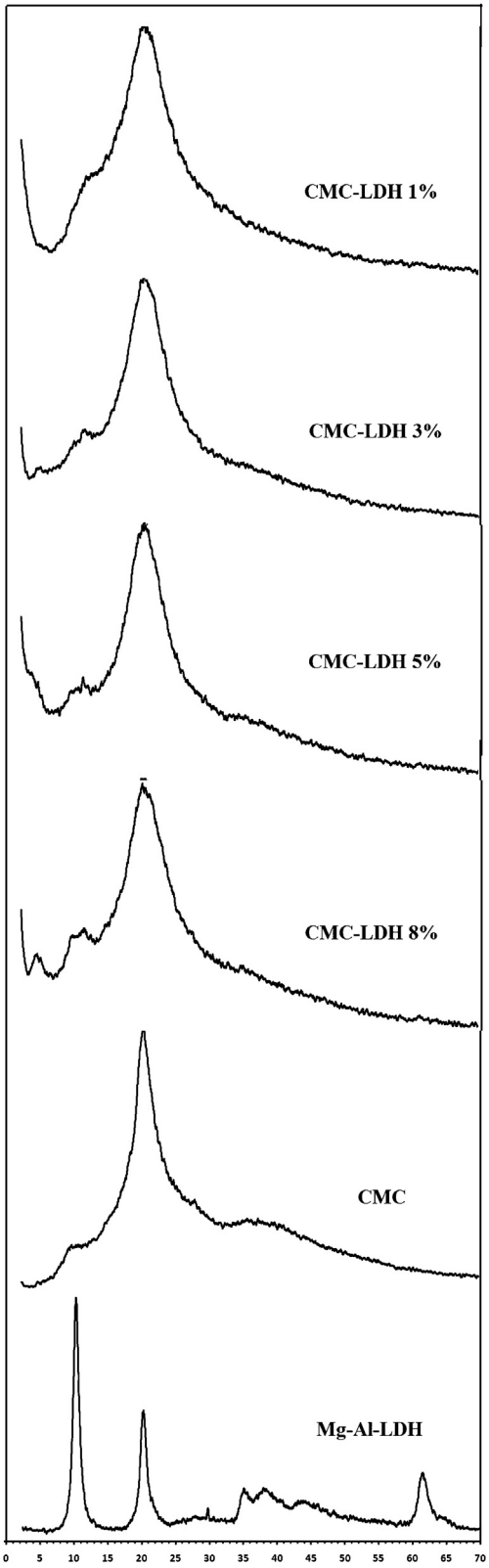

Fig. 2. X-ray diffraction patterns of CMC film, Mg–Al-LDH and CMC–LDH nanocomposite films.

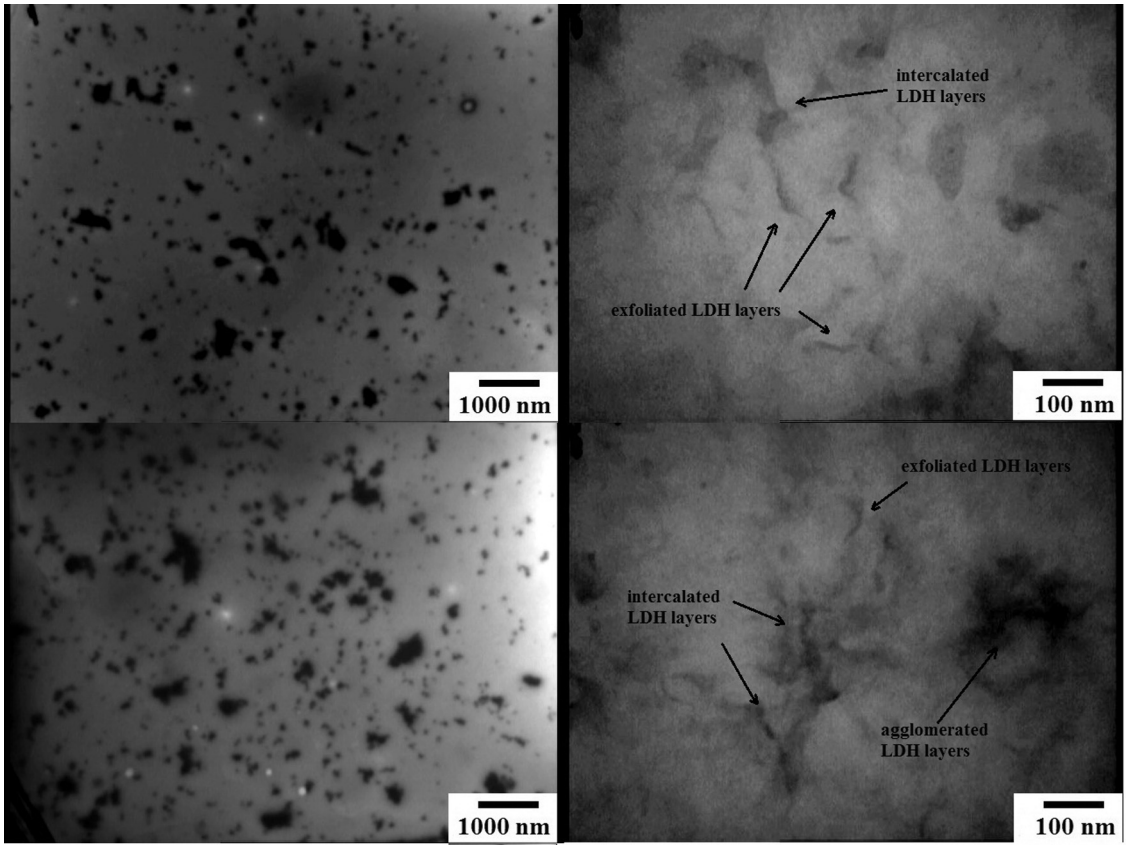

Fig. 3. TEM images of the CMC–LDH nanocomposite film with 3 wt% LDH (a and b) and 8 wt% LDH (c and d) at low and high magnification, respectively.

3.2. The XRD spectrum

The XRD spectrum of synthesized LDH and CMC–LDH nanocomposite films containing 1, 3, 5, and 8 wt.% of LDH) in the 2θ range of 2°–70° are shown in Fig. 2. The XRD spectrum of synthesized Mg-Al LDH shows that the obtained material is highly crystalline and has a layered geometry. The main diffraction peak of Mg–Al-LDH is obtained at 2θ value of 10.26°, which correspond to a (0 0 3) spacing of pristine LDH. This peak demonstrates the formation of LDH. The d-spacing value of Mg–Al-LDH is calculated as 0.862 by using Bragg's equation. XRD pattern of CMC and CMC–LDH nanocomposite films provide a weak peak at $2\theta \sim 11^\circ$ and a strong peak at $2\theta \sim 20^\circ$ (Fig. 2), that are typical of CMC (Uskoković, 2008). The absence of the diffraction peaks corresponding to the LDH, confirms the formation of nanocomposites or disordered systems. It can be seen that for CMC–LDH nanocomposites with 8 and 5 wt% LDH, a new broad peak is appears at 2θ values of 5° and 3.5° with d_{003} basal spacing of 1.77 and 2.53 nm, respectively. This weak broad peak is indicative of an exfoliated/intercalated nanostructure for CMC–LDH nanocomposites with 8 and 5 wt% LDH loading. When the LDH content is below 5 wt%, no diffraction peak can be observed in $2\theta = 2^\circ - 10^\circ$. These data illustrate that fully exfoliated CMC–LDH nanocompsite structures can be obtained by decreasing LDH content to below 5 wt.%.

3.3. TEM analysis

Although, XRD is a powerful and essential apparatus for evaluating the microstructure of nanocomposites, TEM instrument is the best direct evidence to describe the morphology and visualize the exact intercalation or exfoliation degree of filler in the polymeric nanocomposites. Fig. 3 illustrates the bright-field TEM micrographs for CMC–LDH nanocomposites with 3 and 8 wt.% LDH content at low (left) and high (right) magnifications. The dark areas represent the LDHs and the gray areas represent the CMC matrix. As it can be seen in Fig. 3a and c, the LDH layers exist as individual layers or agglomerated particles with particle size about 100 nm. TEM results showed that the LDH particles were well dispersed in the CMC matrix at LDH contents less than 8 wt%. This is also confirmed by the XRD patterns of the CMC–LDH nanocomposites (see Fig. 2), in which the characteristic peaks of the LDH are absent. Therefore, the CMC–LDH nanocomposites were prepared successfully by solution mixing. Nonetheless, the LDH tended to aggregate when the LDH content was increased to 8 wt%.

From the TEM observations at high magnification (Fig. 3b and d), clearly the delaminating took place resulting in the presence of exfoliated LDH layers. In addition to the exfoliated LDH layers, some intercalated structures are also observed in the image. Moreover, some black points are obvious in the image, regarding the agglomerates of LDH layers, which suggests the existence of non-exfoliated structure. The image shows only a small area of intercalated and agglomerated LDH layers for LDH content of 3 wt% but larger intercalated and agglomerated areas for LDH content of 8 wt%. In summary, it could be said that the morphological features of the prepared CMC–LDH nanocomposites is composed of highly exfoliated LDH layers, including the intercalated regions as well as agglomerated regions.

3.4. SEM analysis

SEM analysis was carried out for investigate the microstructure and surface morphology of neat CMC film and CMC–LDH nanocomposite films. SEM images of surface of the neat CMC and CMC–LDH nanocomposite films are shown in Fig. 4. As it can be seen in Fig. 4a,

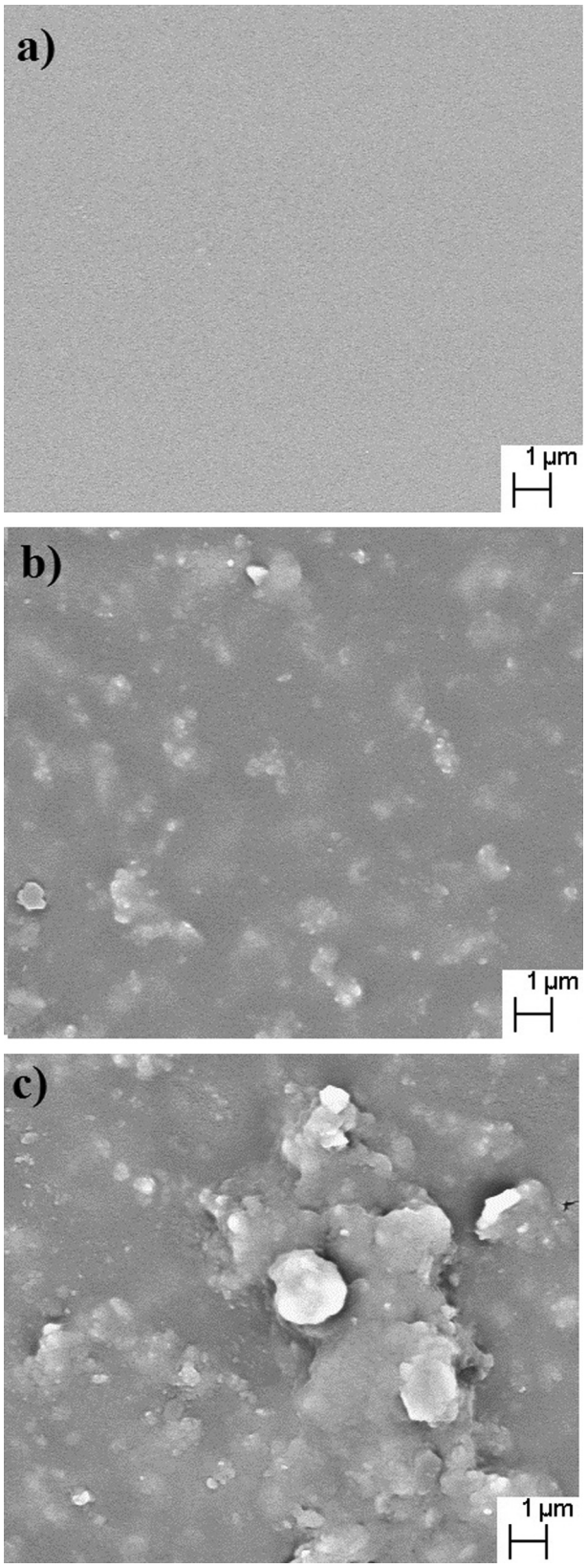

Fig. 4. SEM images of (a) CMC film (b) the CMC–LDH nanocomposite film with 3 wt% and (c) CMC–LDH nanocomposite film with 8 wt% LDH.

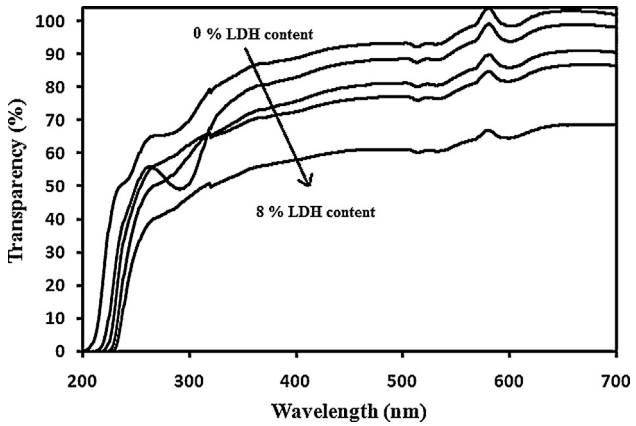

Fig. 5. Visible-light transmittance of pure CMC film and CMC–LDH nanocomposite films.

neat CMC film revealed a very homogenous and smooth surface. Nevertheless, the homogeneity and smoothness of the films' surface decreased with the addition of LDH particles (see Fig. 4b and c). SEM results showed that the LDH particles were well dispersed in the CMC matrix at 3 wt% LDH content. Meanwhile, some aggregation can be seen for the nanocomposite containing the highest content (8 wt%) of LDH particles. These results are in good agreement with TEM results.

3.5. Optical behavior of the CMC–LDH nanocomposite films

Fig. 5 illustrates the influence of LDHs on the transparency of CMC–LDH nanocomposite films in the wavelength region of 400–700 nm. As expected, incorporation of the LDHs into the CMC matrix is accompanied by a decrease in the film transparency, which is proportional to the weight percentage of the filler. The nanocomposite films with LDH content below 8 wt% exhibited an optical transmission higher than 70% under the visible-light region. The optical transmission was notably decreased for nanocomposite films with 8 wt% LDH content leading a transmission of 55%. At high LDH content, the LDH particles could not be completely exfoliated and dispersed into the polymeric matrix and some remained as aggregates, which reduce the transparency of the films.

3.6. Water vapor permeability (WVP) of CMC–LDH nanocomposite films

Fig. 6 shows the influence of LDH concentration on the WVP of the CMC–LDH nanocomposite films. As it can be seen in the figure, a reduction in the WVP values of films with the increase of the LDH concentration is observed. The WVP values of nanocomposite films decreased by 13–37% depending on the LDH concentration. The

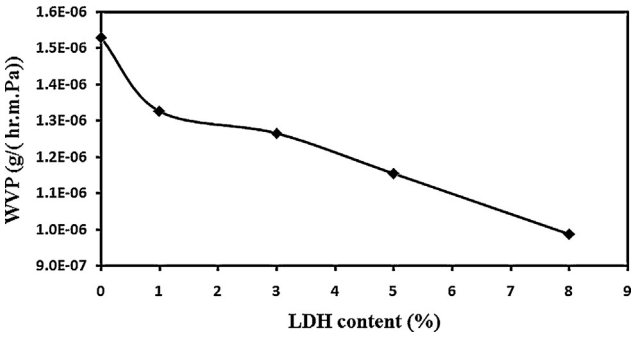

Fig. 6. Effect of LDH content (wt%) on water vapor permeability of CMC-based films.

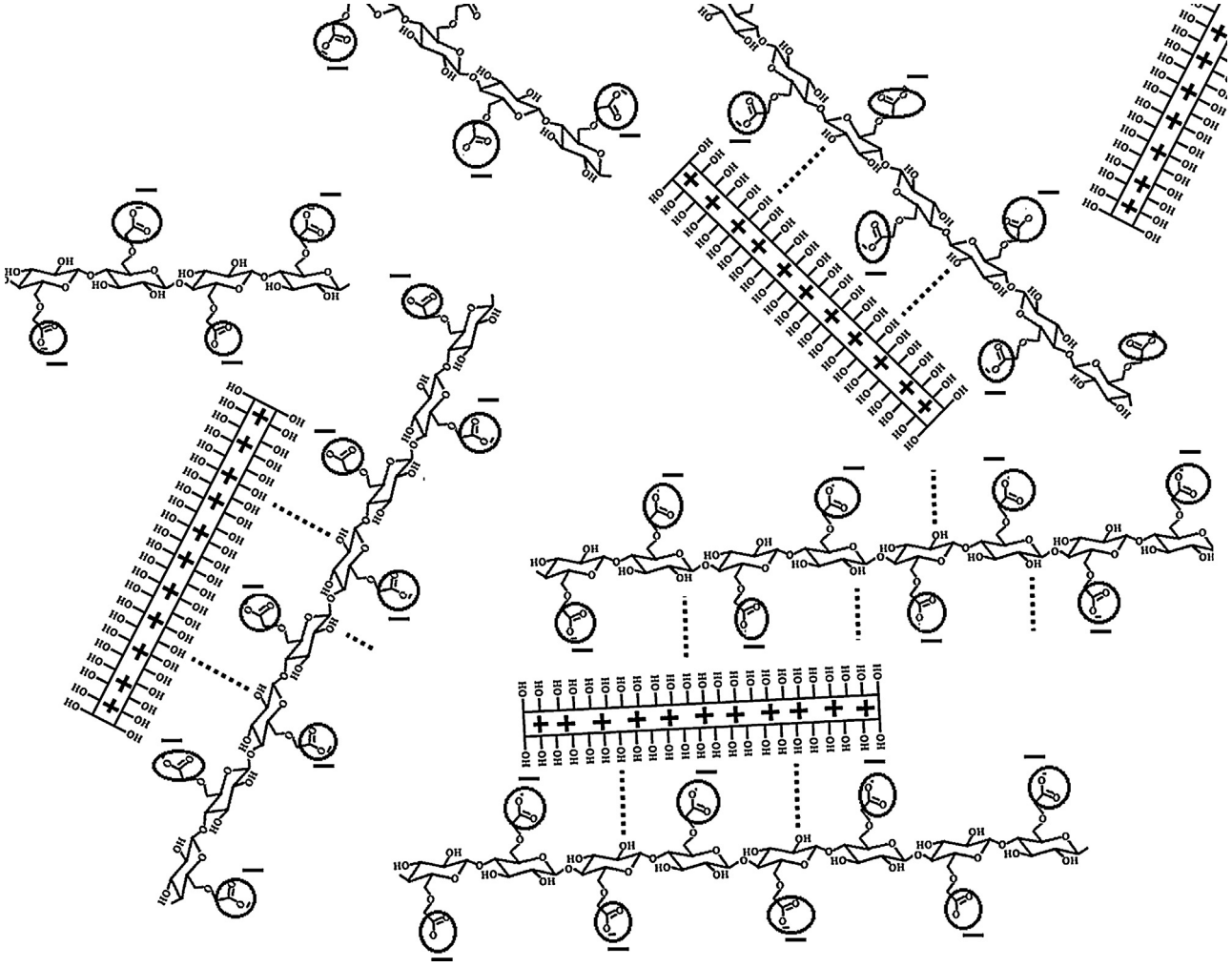

Scheme 1. Schematic illustration of the possible interaction of LDH particles with the CMC chains.

dramatic decrease in the water vapor permeability of CMC–LDH nanocomposite films is attributed to the concept of tortuous paths. In the presence of ordered and dispersed impermeable LDH layers the permeating water molecules are forced to follow longer and more tortuous pathways to diffuse through the nanocomposite (Choudalakis & Gotsis, 2009; Tunc et al., 2007).

3.7. Mechanical properties of CMC–LDH nanocomposite films

Fig. 7 illustrates the mechanical properties of the CMC–LDH nanocomposite films as a function of LDH content. Fig. 7a and b show the effect of LDH content on the tensile strength and tensile modulus of CMC-based films. It is obvious that both the tensile strength and tensile modulus of films increase with the increase of the LDH content. When the LDH contents varied from 0 to 3 wt%, the tensile strength increased from 10.33 to 25.65 MPa (an increase of 148% compared with the pure CMC film), and the tensile modulus increased from 427 to 1040 MPa (an increase of 143% compared with the pure CMC film). Here LDH sheets act as reinforcing agent for CMC-based films and causes higher tensile strength and tensile modulus values. These results provided evidence of stress transfer between CMC and LDH sheets and an increased toughness for the nanocomposite films.

The improvement of tensile strength and tensile modulus was attributed to the strong interfacial adhesion of LDH with CMC (Huang et al., 2011; Kang et al., 2009; Moreira, Pedro, Glenn, Marconcini, & Mattoso, 2013). A proposed structure for the CMC–LDH nanocomposites is schematically illustrated in Scheme 1. Scheme 1 1illustrates the strong electrostatic attraction between positively charged LDH layers and negatively charged carboxylate moieties on CMC chain and as well as hydrogen bonding between hydroxyl groups of the CMC chains and the exposed hydroxyl groups on the surface of LDH sheets. The LDH sheets encapsulated by CMC chains are in a stable exfoliated state.

Conversely, when the LDH content increased to 8 wt%, the tensile strength and tensile modulus of the nanocomposite films decreased to 17.79 and 950 MPa, respectively. This is attributed to the agglomeration of LDH particles, as shown in Fig. 3c and d, and as a result reducing the effectiveness of filler loading (Wu et al., 2011). Fig. 7c indicates the effect of LDH content on the elongation at break values of the films. The elongation at break value of the neat CMC film was found to be 17.2%. As it can be seen, the elongation at break values of the films decreases with the increase of LDH content. It indicates that the nanocomposites become more brittle, compared with neat CMC film. A significant decrease down to 6.7% in the elongation at break value of the CMC nanocomposite films was observed for films having a 3% LDH content, which represents a relative decrease of 61% compared to that of the control sample. At a higher LDH content (8%), the elongation at break of CMC nanocomposite film dropped to 1.9%. It is speculated that, higher amount of agglomerated LDH formed when more LDH existed, leading to a significant decrease of elongation property. Generally, polymer/clay

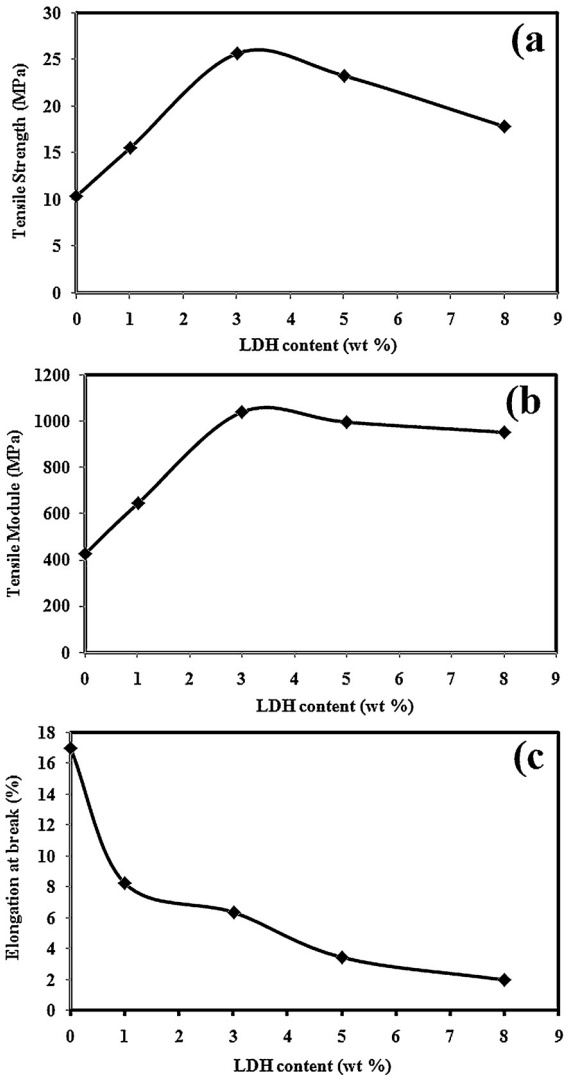

Fig. 7. Effect of LDH content (wt%) on (a) tensile strength (b) tensile modulus and (c) elongation at break of CMC-based films.

nanocomposites are much more brittle than neat polymers and have higher tensile strength, tensile modulus and lower elongation at break (Pavlidou & Papaspyrides, 2008).

4. Conclusions

Carboxymethyl cellulose/layered double hydroxide (CMC–LDH) nanocomposite films with LDH concentration up to 8 wt% were successfully prepared by solution casting of CMC and Mg–Al-LDH in water. Structural details were provided by FTIR, XRD, TEM and SEM analysis. XRD and TEM results demonstrated that the LDH particles were well dispersed in CMC matrix at 3 wt% LDH content and formation of exfoliated structure. Nevertheless, at LDH contents higher than 3 wt%, nanocomposite revealed an intercalated structure and LDH particles tended to be slightly aggregate. Incorporation of the LDHs into the CMC matrix is accompanied by a decrease in the film transparency. The addition of LDH particles caused a significant reduction in the water vapor permeability (WVP) of the CMC-based nanocomposite films. With addition of 8 wt% LDH into the CMC matrix, the WVP of CMC was decreased by 37%. Incorporation of LDH particles significantly improved the mechanical properties of CMC-based films. Mechanical test showed that the tensile strength 25.65 MPa of the CMC–LDH nanocomposite film with 3 wt% LDH is 148% higher than those of pure CMC film, while its tensile modulus 1040 MPa is 143% higher than those of pure CMC film. The improvement of tensile strength and tensile modulus was related to the strong interaction of LDH sheets with CMC chains. But, a decrease in the tensile strength and tensile modulus was observed when the LDH content increased up to 3 wt%. The elongation at break values of the films decreased with the increase of LDH content due to increasing brittleness of films.

Acknowledgments

We would like to thank Department of Physics in the University of Tabriz for XRD analysis. Authors also gratefully acknowledge the University of Tabriz (S/27/3243-29) for the financial supports of this work.

References

Alcantara, A. C. S., Aranda, P., Darder, M., & Ruiz-Hitzky, E. (2010). Bionanocomposites based on alginate–zein/layered double hydroxide materials as drug delivery systems. *Journal of Materials Chemistry*, *20*(42), 9495–9504.

Basta, A. H., & El-Saied, H. (2008). New approach for utilization of cellulose derivatives metal complexes in preparation of durable and permanent colored papers. *Carbohydrate Polymers*, *74*(2), 301–308.

Bitinis, N., Fortunati, E., Verdejo, R., Bras, J., Kenny, J. M., Torre, L., et al. (2013). Poly (lactic acid)/natural rubber/cellulose nanocrystal bionanocomposites Part II. Properties evaluation. *Carbohydrate Polymers*, *96*(2), 621–627.

Chang, P. R., Yu, J., Ma, X., & Anderson, D. P. (2011). Polysaccharides as stabilizers for the synthesis of magnetic nanoparticles. *Carbohydrate Polymers*, *83*(2), 640–644.

Chen, L., Goren, B. K., Ozisik, R., & Schadler, L. S. (2012). Controlling bubble density in MWNT/polymer nanocomposite foams by MWNT surface modification. *Composites Science and Technology*, *72*(2), 190–196.

Choi, Y., & Simonsen, J. (2006). Cellulose nanocrystal-filled carboxymethyl cellulose nanocomposites. *Journal of Nanoscience and Nanotechnology*, *6*(3), 633–639.

Choudalakis, G., & Gotsis, A. D. (2009). Permeability of polymer/clay nanocomposites: A review. *European Polymer Journal*, *45*(4), 967–984.

Choy, J. H., Kwak, S. Y., Park, J. S., Jeong, Y. J., & Portier, J. (1999). Intercalative nanohybrids of nucleoside monophosphates and DNA in layered metal hydroxide. *Journal of the American Chemical Society*, *121*(6), 1399–1400.

Chung, Y. L., & Lai, H. M. (2010). Preparation and properties of biodegradable starch-layered double hydroxide nanocomposites. *Carbohydrate Polymers*, *80*(2), 525–532.

Darder, M., López-Blanco, M., Aranda, P., Leroux, F., & Ruiz-Hitzky, E. (2005). Bionanocomposites based on layered double hydroxides. *Chemistry of Materials*, *17*(8), 1969–1977.

Desigaux, L., Belkacem, M. B., Richard, P., Cellier, J., Léone, P., Cario, L., et al. (2006). Self-assembly and characterization of layered double hydroxide/DNA hybrids. *Nano Letters*, *6*(2), 199–204.

Eichhorn, S. J. (2011). Cellulose nanowhiskers: Promising materials for advanced applications. *Soft Matter*, *7*(2), 303–315.

El Achaby, M., Arrakhiz, F. E., Vaudreuil, S., el Kacem Qaiss, A., Bousmina, M., & Fassi-Fehri, O. (2012). Mechanical, thermal, and rheological properties of graphene-based polypropylene nanocomposites prepared by melt mixing. *Polymer Composites*, *33*(5), 733–744.

Galpaya, D., Wang, M., Liu, M., Motta, N., Waclawik, E. R., & Yan, C. (2012). Recent advances in fabrication and characterization of graphene-polymer nanocomposites. *Graphene*, *1*(2), 30–49.

Gorrasi, G., Bugatti, V., & Vittoria, V. (2012). Pectins filled with LDH-antimicrobial molecules: Preparation, characterization and physical properties. *Carbohydrate Polymers*, *89*(1), 132–137.

Heinze, T., Liebert, T., Klüfers, P., & Meister, F. (1999). Carboxymethylation of cellulose in unconventional media. *Cellulose*, *6*(2), 153–165.

Huang, S., Cen, X., Zhu, H., Yang, Z., Yang, Y., Tjiu, W. W., et al. (2011). Facile preparation of poly (vinyl alcohol) nanocomposites with pristine layered double hydroxides. *Materials Chemistry and Physics*, *130*(3), 890–896.

Kang, H., Huang, G., Ma, S., Bai, Y., Ma, H., Li, Y., et al. (2009). Coassembly of inorganic macromolecule of exfoliated LDH nanosheets with cellulose. *Journal of Physical Chemistry C*, *113*(21), 9157–9163.

Kuang, Y., Zhao, L., Zhang, S., Zhang, F., Dong, M., & Xu, S. (2010). Morphologies, preparations and applications of layered double hydroxide micro-/nanostructures. *Materials*, *3*(12), 5220–5235.

Leroux, F., Gachon, J., & Besse, J. P. (2004). Biopolymer immobilization during the crystalline growth of layered double hydroxide. *Journal of Solid State Chemistry*, *177*(1), 245–250.

Luna-Martinez, J. F., Hernández-Uresti, D. B., Reyes-Melo, M. E., Guerrero-Salazar, C. A., González-González, V. A., & Sepulveda-Guzman, S. (2011). Synthesis and optical characterization of ZnS–sodium carboxymethyl cellulose nanocomposite films. *Carbohydrate Polymers*, *84*(1), 566–570.

Mandal, S., Patil, V. S., & Mayadevi, S. (2012). Alginate and hydrotalcite-like anionic clay composite systems: Synthesis, characterization and application studies. *Microporous and Mesoporous Materials*, *158*, 241–246.

Moreira, F. K., Pedro, D. C., Glenn, G. M., Marconcini, J. M., & Mattoso, L. H. (2013). Brucite nanoplates reinforced starch bionanocomposites. *Carbohydrate Polymers*, *92*, 1743–1751.

Namazi, H., Dadkhah, A., & Mosadegh, M. (2012). New biopolymer nanocomposite of starch-graft polystyrene/montmorillonite clay prepared through emulsion polymerization method. *Journal of Polymers and the Environment*, *20*(3), 794–800.

Namazi, H., Mosadegh, M., & Dadkhah, A. (2009). New intercalated layer silicate nanocomposites based on synthesized starch-g-PCL prepared via solution intercalation and in situ polymerization methods: As a comparative study. *Carbohydrate Polymers*, *75*(4), 665–669.

Oh, J. M., Kwak, S. Y., & Choy, J. H. (2006). Intracrystalline structure of DNA molecules stabilized in the layered double hydroxide. *Journal of Physics and Chemistry of Solids*, *67*(5), 1028–1031.

Olanrewaju, J., Newalkar, B. L., Mancino, C., & Komarneni, S. (2000). Simplified synthesis of nitrate form of layered double hydroxide. *Materials Letters*, *45*(6), 307–310.

Pavlidou, S., & Papaspyrides, C. D. (2008). A review on polymer–layered silicate nanocomposites. *Progress in Polymer Science*, *33*(12), 1119–1198.

Ruiz-Hitzky, E., Darder, M., Aranda, P., & Ariga, K. (2010). Advances in biomimetic and nanostructured biohybrid materials. *Advanced Materials*, *22*(3), 323–336.

Shawky, H. A., Chae, S. R., Lin, S., & Wiesner, M. R. (2011). Synthesis and characterization of a carbon nanotube/polymer nanocomposite membrane for water treatment. *Desalination*, *272*(1), 46–50.

Shen, J., Song, Z., Qian, X., & Yang, F. (2010). Carboxymethyl cellulose/alum modified precipitated calcium carbonate fillers: Preparation and their use in papermaking. *Carbohydrate Polymers*, *81*(3), 545–553.

Singh, V., & Ahmad, S. (2012). Synthesis and characterization of carboxymethyl cellulose-silver nanoparticle (AgNp)-silica hybrid for amylase immobilization. *Cellulose*, *19*(5), 1759–1769.

Song, J., Birbach, N. L., & Hinestroza, J. P. (2012). Deposition of silver nanoparticles on cellulosic fibers via stabilization of carboxymethyl groups. *Cellulose*, *19*(2), 411–424.

Stigsson, V., Kloow, G., & Germgård, U. (2006). The influence of the solvent system used during manufacturing of CMC. *Cellulose*, *13*(6), 705–712.

Tunc, S., Angellier, H., Cahyana, Y., Chalier, P., Gontard, N., & Gastaldi, E. (2007). Functional properties of wheat gluten/montmorillonite nanocomposite films processed by casting. *Journal of Membrane Science*, *289*(1), 159–168.

Uskoković, V. (2008). Composites comprising cholesterol and carboxymethyl cellulose. *Colloids and Surfaces B: Biointerfaces*, *61*(2), 250–261.

Wang, J., & Somasundaran, P. (2005). Adsorption and conformation of carboxymethyl cellulose at solid–liquid interfaces using spectroscopic, AFM and allied techniques. *Journal of Colloid and Interface Science*, *291*(1), 75–83.

Wang, Q., & O'Hare, D. (2012). Recent advances in the synthesis and application of layered double hydroxide (LDH) nanosheets. *Chemical Reviews*, *112*(7), 4124–4155.

Wu, D., Chang, P. R., & Ma, X. (2011). Preparation and properties of layered double hydroxide–carboxymethylcellulose sodium/glycerol plasticized starch nanocomposites. *Carbohydrate Polymers*, *86*(2), 877–882.

Yadav, M., Rhee, K. Y., Jung, I. H., & Park, S. J. (2013). Eco-friendly synthesis, characterization and properties of a sodium carboxymethyl cellulose/graphene oxide nanocomposite film. *Cellulose*, *20*(2), 687–698.

Yadollahi, M., & Namazi, H. (2013). Synthesis and characterization of carboxymethyl cellulose/layered double hydroxide nanocomposites. *Journal of Nanoparticle Research*, *15*(4), 1–9.

Yang, X. H., & Zhu, W. L. (2007). Viscosity properties of sodium carboxymethylcellulose solutions. *Cellulose*, *14*(5), 409–417.

Yu, B., Bian, H., & Plank, J. (2010). Self-assembly and characterization of Ca–Al–LDH nanohybrids containing casein proteins as guest anions. *Journal of Physics and Chemistry of Solids*, *71*(4), 468–472.

Zakharov, N. A., Ezhova, Z. A., Kalinnikov, V. T., & Chalykh, A. E. (2005). Hydroxyapatite-carboxymethyl cellulose nanocomposite biomaterial. *Inorganic Materials*, *41*(5), 509–515.

Zhao, R., Torley, P., & Halley, P. J. (2008). Emerging biodegradable materials: Starch- and protein-based bio-nanocomposites. *Journal of Materials Science*, *43*(9), 3058–3071.

Zümreoglu-Karan, B., & Ay, A. N. (2012). Layered double hydroxides – Multifunctional nanomaterials. *Chemical Papers*, *66*(1), 1–10.